A high-order non-conforming discontinuous Galerkin method for time-domain electromagnetics

Hassan Fahs, Stephane Lanteri

A high-order non-conforming discontinuous Galerkin method for time-domain electromagnetics

Hassan Fahs [a],[*], Stéphane Lanteri [a]

[a]*INRIA, 2004 Route des Lucioles, BP 93, F-06902 Sophia Antipolis Cedex, France*

Abstract

In this paper, we discuss the formulation, stability and validation of a high-order non-dissipative discontinuous Galerkin (DG) method for solving Maxwell's equations on non-conforming simplex meshes. The proposed method combines a centered approximation for the numerical fluxes at inter element boundaries, with either a second-order or a fourth-order leap-frog time integration scheme. Moreover, the interpolation degree is defined at the element level and the mesh is refined locally in a non-conforming way resulting in arbitrary-level hanging nodes. The method is proved to be stable and conserves a discrete counterpart of the electromagnetic energy for metallic cavities. Numerical experiments with high-order elements show the potential of the method.

Key words: computational electromagnetism, time-domain Maxwell's equations, discontinuous Galerkin method, explicit time integration, non-conforming meshes

1 Introduction

Time domain solutions of Maxwell's equations find applications in the applied sciences and engineering problems such as the design and optimization of antennas and radars, the design of emerging technologies (high speed electronics, integrated optics, etc.), the study of human exposure to electromagnetic waves [8], to name a few. These problems require high fidelity approximate solutions with a rigorous control of the numerical errors. Even for linear problems such conditions force one to look beyond standard computational techniques and

---

[*] Corresponding author.
   Email address: Hassan.Fahs@gmail.com (Hassan Fahs).

seek new numerical frameworks enabling the accurate, efficient, and robust modeling of wave phenomena over long simulation times in settings of realistic geometrical complexity.

The finite difference time-domain (FDTD) method, first introduced by Yee in 1966 [13] and later developed by Taflove and others [10], has been used for a broad range of applications in computational electromagnetics. In spite of its flexibility and second-order accuracy in a homogeneous medium, the Yee scheme suffers from serious accuracy degradation when used to model complex geometries. In recent years, a number of efforts aimed at addressing the shortcomings of the classical FDTD scheme, *e.g.* embedding schemes to overcome staircasing [12], high-order finite difference schemes [10]-[14], non-conforming orthogonal FDTD methods [2]. Most of these methods, however, have not really penetrated into main stream user community, partly due to their complicated nature and partly because these methods themselves often introduce other complications.

The discontinuous Galerkin methods enjoy an impressive favor nowadays and are now used in various applications. Being higher order versions of traditional finite volume methods [6], discontinuous Galerkin time-domain (DGTD) methods based on discontinuous finite element spaces, easily handle elements of various types and shapes, irregular non-conforming meshes [4], and even locally varying polynomial degree. They hence offer great flexibility in the mesh design, but also lead to (block-) diagonal mass matrices and therefore yield fully explicit, inherently parallel methods when coupled with explicit time stepping [1]. Moreover, continuity is weakly enforced across mesh interfaces by adding suitable bilinear forms (so-called numerical fluxes) to the standard variational formulations. Whereas high-order discontinuous Galerkin time-domain methods have been developed on conforming hexahedral [3] and tetrahedral [5] meshes, the design of non-conforming discontinuous Galerkin time-domain methods is still in its infancy. In practice, the non-conformity can result from a local refinement of the mesh (*i.e. h*-refinement), of the interpolation degree (*i.e. p*-enrichment) or of both of them (*i.e. hp*-refinement).

In this paper, we present a high-order DGTD method on non-conforming simplicial meshes. It is an extension of the DG formulation recently studied in [4]. One of the most important properties which should be aimed at is the conservation of a discrete counterpart of the electromagnetic energy on a general non-conforming simplex mesh with arbitrary level hanging nodes, including *hp*-type refinement. This cannot be obtained with DG methods based on upwind fluxes [7]. The rest of the paper is organized as follows. In section 2, we introduce the high-order non-conforming DGTD method for solving the first-order Maxwell equations, based on totally centered fluxes and a high-order leap-frog time integration scheme. We prove the stability of the resulting fully discretized scheme and its energy conservation properties in section 3. The stability result is more general than the ones obtained in [4]-[5]. Numerical

results are presented in section 4. Finally, section 5 concludes this paper and states future research directions.

2 Discontinuous Galerkin Time-Domain method

We consider the Maxwell equations in three space dimensions for heterogeneous anisotropic linear media with no source. The electric permittivity tensor $\bar{\bar{\epsilon}}(x)$ and the magnetic permeability tensor $\bar{\bar{\mu}}(x)$ are varying in space, time-invariant and both symmetric positive definite. The electric field $\vec{\mathbf{E}} = {}^{t}(E_x, E_y, E_z)$ and the magnetic field $\vec{\mathbf{H}} = {}^{t}(H_x, H_y, H_z)$ verify:

$$\bar{\bar{\epsilon}}\partial_t\vec{\mathbf{E}} = \operatorname{curl}\vec{\mathbf{H}}, \quad \bar{\bar{\mu}}\partial_t\vec{\mathbf{H}} = -\operatorname{curl}\vec{\mathbf{E}}, \tag{1}$$

where the symbol ∂_t denotes a time derivative. These equations are set and solved on a bounded polyhedral domain Ω of $\mathbb{R}^3$. For the sake of simplicity, a metallic boundary condition is set everywhere on the domain boundary $\partial\Omega$, *i.e.* $\vec{n} \times \vec{\mathbf{E}} = 0$ (where $\vec{n}$ denotes the unitary outwards normal).

We consider a partition Ω_h of Ω into a set of tetrahedra τ_i of size $h_i = \operatorname{diam}(\tau_i)$ with boundaries $\partial\tau_i$ such that $h = \max_{\tau_i \in \Omega_h} h_i$. To each $\tau_i \in \Omega_h$ we assign an integer $p_i \geq 0$ (the local interpolation order) and we collect the p_i in the vector $p = \{p_i : \tau_i \in \Omega_h\}$. Of course, if p_i is uniform in all element τ_i of the mesh, we have $p = p_i$. Within this construction we admit meshes with possibly hanging nodes *i.e.* by allowing non-conforming (or irregular) meshes where element vertices can lie in the interior of faces of other elements. Each tetrahedron τ_i is assumed to be the image, under a smooth bijective (diffeomorphic) mapping, of a fixed reference tetrahedron $\hat{\tau} = \{\hat{x}, \hat{y}, \hat{z}|\ \hat{x}, \hat{y}, \hat{z} \geq 0; \hat{x} + \hat{y} + \hat{z} \leq 1\}$. For each τ_i, V_i denotes its volume, and $\bar{\bar{\epsilon}}_i$ and $\bar{\bar{\mu}}_i$ are respectively the local electric permittivity and magnetic permeability tensors of the medium, which could be varying inside the element τ_i. For two distinct tetrahedra τ_i and τ_k in Ω_h, the intersection $\tau_i \cap \tau_k$ is a triangle a_{ik} which we will call interface, with unitary normal vector $\vec{n}_{ik}$, oriented from τ_i towards τ_k. For the boundary interfaces, the index k corresponds to a fictitious element outside the domain. Finally, we denote by $\mathcal{V}_i$ the set of indices of the elements which are neighbors of τ_i (having an interface in common). We also define the perimeter P_i of τ_i by $P_i = \sum_{k\in\mathcal{V}_i} \mathbf{s}_{ik}$. We have the following geometrical property for all elements: $\sum_{k\in\mathcal{V}_i} \mathbf{s}_{ik}\vec{n}_{ik} = 0$.

In the following, for a given partition Ω_h and vector p, we seek approximate solutions to (1) in the finite dimensional subspace $V_p(\Omega_h) := \{\vec{v} \in L^2(\Omega)^3 : \vec{v}_{|\tau_i} \in \mathbb{P}_{p_i}(\tau_i),\ \forall\tau_i \in \Omega_h\}$, where $\mathbb{P}_{p_i}(\tau_i)$ denotes the space of nodal polynomials

of degree at most p_i inside the element τ_i. Note that the polynomial degree, p_i, may vary from element to element in the mesh. By non-conforming interface we mean an interface a_{ik} for which at least one of its vertices is a hanging node or/and such that $p_{i|a_{ik}} \neq p_{k|a_{ik}}$.

According to the discontinuous Galerkin approach, the electric and magnetic fields inside each finite element are linear combinations $(\vec{\mathbf{E}}_i, \vec{\mathbf{H}}_i)$ of linearly independent basis vector fields $\vec{\varphi}_{ij}$, $1 \leq j \leq d_i$, where d_i denotes the local number of degrees of freedom (DOF) inside τ_i. We denote by $\mathcal{P}_i = \mathrm{Span}(\vec{\varphi}_{ij}, \ 1 \leq j \leq d_i)$. The approximate fields $(\vec{\mathbf{E}}_h, \vec{\mathbf{H}}_h)$, defined by $(\forall i, \vec{\mathbf{E}}_{h|\tau_i} = \vec{\mathbf{E}}_i, \vec{\mathbf{H}}_{h|\tau_i} = \vec{\mathbf{H}}_i)$ are allowed to be completely discontinuous across element boundaries. For such a discontinuous field $\vec{\mathbf{U}}_h$, we define its average $\{\vec{\mathbf{U}}_h\}_{ik}$ through any internal interface a_{ik}, as $\{\vec{\mathbf{U}}_h\}_{ik} = (\vec{\mathbf{U}}_{i|a_{ik}} + \vec{\mathbf{U}}_{k|a_{ik}})/2$. Note that for any internal interface a_{ik}, $\{\vec{\mathbf{U}}_h\}_{ki} = \{\vec{\mathbf{U}}_h\}_{ik}$. Because of this discontinuity, a global variational formulation cannot be obtained. However, dot-multiplying (1) by any given vector function $\vec{\varphi} \in \mathcal{P}_i$, integrating over each single element τ_i and integrating by parts, yields:

$$
\begin{cases}
\displaystyle \int_{\tau_i} \vec{\varphi} \cdot \bar{\bar{\epsilon}}_i \partial_t \vec{\mathbf{E}} \ = \int_{\tau_i} \mathrm{curl}\,\vec{\varphi} \cdot \vec{\mathbf{H}} - \int_{\partial \tau_i} \vec{\varphi} \cdot (\vec{\mathbf{H}} \times \vec{n}), \\[4mm]
\displaystyle \int_{\tau_i} \vec{\varphi} \cdot \bar{\bar{\mu}}_i \partial_t \vec{\mathbf{H}} = - \int_{\tau_i} \mathrm{curl}\,\vec{\varphi} \cdot \vec{\mathbf{E}} + \int_{\partial \tau_i} \vec{\varphi} \cdot (\vec{\mathbf{E}} \times \vec{n}).
\end{cases}
\tag{2}
$$

In equations (2), we now replace the exact fields $\vec{\mathbf{E}}$ and $\vec{\mathbf{H}}$ by the approximate fields $\vec{\mathbf{E}}_h$ and $\vec{\mathbf{H}}_h$ in order to evaluate volume integrals. For integrals over $\partial \tau_i$, a specific treatment must be introduced since the approximate fields are discontinuous through element faces. We choose to use completely centered fluxes, $i.e.\ \forall i, \forall k \in \mathcal{V}_i, \ \vec{\mathbf{E}}_{|a_{ik}} \simeq \{\vec{\mathbf{E}}_h\}_{ik}, \ \vec{\mathbf{H}}_{|a_{ik}} \simeq \{\vec{\mathbf{H}}_h\}_{ik}$. The metallic boundary condition on a boundary interface a_{ik} (k in the element index of the fictitious neighboring element) is dealt with *weakly*, in the sense that traces of fictitious fields $\vec{\mathbf{E}}_k$ and $\vec{\mathbf{H}}_k$ are used for the computation of numerical fluxes for the boundary element τ_i. In the present case, where all boundaries are metallic, we simply take $\vec{\mathbf{E}}_{k|a_{ik}} = -\vec{\mathbf{E}}_{i|a_{ik}}$ and $\vec{\mathbf{H}}_{k|a_{ik}} = \vec{\mathbf{H}}_{i|a_{ik}}$. Replacing surface integrals using centered fluxes in (2) and re-integrating by parts yields:

$$
\begin{cases}
\displaystyle \int_{\tau_i} \vec{\varphi} \cdot \bar{\bar{\epsilon}}_i \partial_t \vec{\mathbf{E}}_i \ = \ \frac{1}{2} \int_{\tau_i} (\mathrm{curl}\,\vec{\varphi} \cdot \vec{\mathbf{H}}_i + \mathrm{curl}\,\vec{\mathbf{H}}_i \cdot \vec{\varphi}) \\[4mm]
\displaystyle \hspace{3.5cm} - \frac{1}{2} \sum_{k \in \mathcal{V}_i} \int_{a_{ik}} \vec{\varphi} \cdot (\vec{\mathbf{H}}_k \times \vec{n}_{ik}), \\[5mm]
\displaystyle \int_{\tau_i} \vec{\varphi} \cdot \bar{\bar{\mu}}_i \partial_t \vec{\mathbf{H}}_i = -\frac{1}{2} \int_{\tau_i} (\mathrm{curl}\,\vec{\varphi} \cdot \vec{\mathbf{E}}_i + \mathrm{curl}\,\vec{\mathbf{E}}_i \cdot \vec{\varphi}) \\[4mm]
\displaystyle \hspace{3.5cm} + \frac{1}{2} \sum_{k \in \mathcal{V}_i} \int_{a_{ik}} \vec{\varphi} \cdot (\vec{\mathbf{E}}_k \times \vec{n}_{ik}).
\end{cases}
\tag{3}
$$

4

We can rewrite this formulation in terms of scalar unknowns. Inside each element, the fields are recomposed according to $\vec{\mathbf{E}}_i = \sum_{1 \leq j \leq d_i} E_{ij} \vec{\varphi}_{ij}$, $\vec{\mathbf{H}}_i = \sum_{1 \leq j \leq d_i} H_{ij} \vec{\varphi}_{ij}$. Let us denote by $\mathbf{E}_i$ and $\mathbf{H}_i$ respectively the column vectors $(E_{il})_{1 \leq l \leq d_i}$ and $(H_{il})_{1 \leq l \leq d_i}$. Equations (3) can be rewritten as:

$$\begin{cases} M_i^\epsilon \partial_t \mathbf{E}_i = K_i \mathbf{H}_i - \sum_{k \in \mathcal{V}_i} S_{ik} \mathbf{H}_k, \\ M_i^\mu \partial_t \mathbf{H}_i = -K_i \mathbf{E}_i + \sum_{k \in \mathcal{V}_i} S_{ik} \mathbf{E}_k, \end{cases} \qquad (4)$$

where the symmetric positive definite mass matrices M_i^σ (σ stands for ϵ or μ), and the symmetric stiffness matrix K_i (all of size d_i) are given by : $(M_i^\sigma)_{jl} = \int_{\tau_i} {}^t\vec{\varphi}_{ij} \cdot \bar{\bar{\sigma}}_i \vec{\varphi}_{il}$ and $(K_i)_{jl} = \dfrac{1}{2} \int_{\tau_i} {}^t\vec{\varphi}_{ij} \cdot \mathrm{curl}\, \vec{\varphi}_{il} + {}^t\vec{\varphi}_{il} \cdot \mathrm{curl}\, \vec{\varphi}_{ij}$. For any interface a_{ik}, the $d_i \times d_k$ rectangular matrix S_{ik} is given by:

$$(S_{ik})_{jl} = \frac{1}{2} \int_{a_{ik}} {}^t\vec{\varphi}_{ij} \cdot (\vec{\varphi}_{kl} \times \vec{n}_{ik}), \quad 1 \leq j \leq d_i, \ 1 \leq l \leq d_k. \qquad (5)$$

Concerning the time discretization, we propose to use a leap-frog (LF$_N$, $N = 2, 4$) scheme. This kind of time scheme has both advantages to be explicit and to be non-dissipative. In the sequel, superscripts refer to time stations and Δt is the fixed time-step. The unknowns related to the electric field are approximated at integer time-stations $t^n = n\Delta t$ and are denoted by $\mathbf{E}_i^n$. The unknowns related to the magnetic field are approximated at half-integer time-stations $t^{n+1/2} = (n+1/2)\Delta t$ and are denoted by $\mathbf{H}_i^{n+1/2}$. The LF$_N$ ($N = 2, 4$) integrator is constructed as follows [15]-[9]:

$$\begin{cases} \mathbf{T}_1 = \Delta t (M_i^\epsilon)^{-1} \mathrm{curl}\, \vec{\mathbf{H}}_i^{n+\frac{1}{2}}, & \mathbf{T}_1^\star = -\Delta t (M_i^\mu)^{-1} \mathrm{curl}\, \vec{\mathbf{E}}_i^{n+1}, \\ \mathbf{T}_2 = -\Delta t (M_i^\mu)^{-1} \mathrm{curl}\, \mathbf{T}_1, & \mathbf{T}_2^\star = \Delta t (M_i^\epsilon)^{-1} \mathrm{curl}\, \mathbf{T}_1^\star, \\ \mathbf{T}_3 = \Delta t (M_i^\epsilon)^{-1} \mathrm{curl}\, \mathbf{T}_2, & \mathbf{T}_3^\star = -\Delta t (M_i^\mu)^{-1} \mathrm{curl}\, \mathbf{T}_2^\star. \\ \\ \mathrm{LF}_2 : \begin{cases} \mathbf{E}_i^{n+1} = \mathbf{E}_i^n + \mathbf{T}_1, \\ \mathbf{H}_i^{n+\frac{3}{2}} = \mathbf{H}_i^{n+\frac{1}{2}} + \mathbf{T}_1^\star. \end{cases} \\ \\ \mathrm{LF}_4 : \begin{cases} \mathbf{E}_i^{n+1} = \mathbf{E}_i^n + \mathbf{T}_1 + \mathbf{T}_3/24, \\ \mathbf{H}_i^{n+\frac{3}{2}} = \mathbf{H}_i^{n+\frac{1}{2}} + \mathbf{T}_1^\star + \mathbf{T}_3^\star/24. \end{cases} \end{cases} \qquad (6)$$

For the treatment of the boundary condition on an interface a_{ik}, we use:

$$\mathbf{E}_{k|a_{ik}}^n = -\mathbf{E}_{i|a_{ik}}^n \ \text{ and } \ \mathbf{H}_{k|a_{ik}}^{n+\frac{1}{2}} = \mathbf{H}_{i|a_{ik}}^{n+\frac{1}{2}}. \qquad (7)$$

3 Stability of the discontinuous Galerkin method

We aim at giving and proving a sufficient condition for the L^2-stability of the proposed discontinuous Galerkin method with only metallic boundary conditions. We use the same kind of energy approach as in [5], where a quadratic form plays the role of a Lyapunov function of the whole set of numerical unknowns. To this end, we suppose that all electric (resp. magnetic) unknowns are gathered in a column vector $\mathbb{E}$ (resp. $\mathbb{H}$) of size $d = \sum_i d_i$, then the space discretized system (4) can be rewritten as:

$$
\begin{cases}
\mathbb{M}^\epsilon \partial_t \mathbb{E} = \mathbb{K}\mathbb{H} - \mathbb{A}\mathbb{H} - \mathbb{B}\mathbb{H}, \\
\mathbb{M}^\mu \partial_t \mathbb{H} = -\mathbb{K}\mathbb{E} + \mathbb{A}\mathbb{E} - \mathbb{B}\mathbb{E},
\end{cases}
\tag{8}
$$

where we have the following definitions and properties:

- $\mathbb{M}^\epsilon, \mathbb{M}^\mu$ and $\mathbb{K}$ are $d \times d$ block diagonal matrices with diagonal blocks equal to M_i^ϵ, M_i^μ and K_i respectively. Therefore $\mathbb{M}^\epsilon$ and $\mathbb{M}^\mu$ are symmetric positive definite matrices, and $\mathbb{K}$ is a symmetric matrix.
- $\mathbb{A}$ is also a $d \times d$ block sparse matrix, whose non-zero blocks are equal to S_{ik} when a_{ik} is an internal interface of the mesh. Since $\vec{n}_{ki} = -\vec{n}_{ik}$, it can be checked from (5) that $(S_{ik})_{jl} = (S_{ki})_{lj}$ and then $S_{ki} = {}^t S_{ik}$; thus $\mathbb{A}$ is a symmetric matrix.
- $\mathbb{B}$ is a $d \times d$ block diagonal matrix, whose non-zero blocks are equal to S_{ik} when a_{ik} is a metallic boundary interface of the mesh. In that case, $(S_{ik})_{jl} = -(S_{ik})_{lj}$, and $S_{ik} = -{}^t S_{ik}$; thus $\mathbb{B}$ is a skew-symmetric matrix.

The discontinuous Galerkin DGTD-$\mathbb{P}_{p_i}$ method using centered fluxes combined with Nth order leap-frog (LF$_N$) time scheme and arbitrary local accuracy and basis functions can be written, in function of the matrix $\mathbb{S} = \mathbb{K} - \mathbb{A} - \mathbb{B}$, in the general form:

$$
\begin{cases}
\mathbb{M}^\epsilon \dfrac{\mathbb{E}^{n+1} - \mathbb{E}^n}{\Delta t} = \mathbb{S}_N \mathbb{H}^{n+\frac{1}{2}}, \\
\mathbb{M}^\mu \dfrac{\mathbb{H}^{n+\frac{3}{2}} - \mathbb{H}^{n+\frac{1}{2}}}{\Delta t} = -{}^t \mathbb{S}_N \mathbb{E}^{n+1},
\end{cases}
\tag{9}
$$

where the matrix $\mathbb{S}_N$ (N being the order of the leap-frog scheme) verifies:

$$
\mathbb{S}_N =
\begin{cases}
\mathbb{S} & \text{if } N = 2, \\
\mathbb{S}(\mathbb{I} - \dfrac{\Delta t^2}{24} \mathbb{M}^{-\mu} {}^t \mathbb{S} \mathbb{M}^{-\epsilon} \mathbb{S}) & \text{if } N = 4.
\end{cases}
\tag{10}
$$

We now define the following discrete version of the electromagnetic energy.

Definition 1 *We consider the following electromagnetic energies inside each tetrahedron τ_i and in the whole domain Ω:*

- *the local energy :* $\forall i, \; \mathcal{E}_i^n = \dfrac{1}{2}(\,{}^t\mathbf{E}_i^n M_i^\epsilon \mathbf{E}_i^n + \,{}^t\mathbf{H}_i^{n-\frac{1}{2}} M_i^\mu \mathbf{H}_i^{n+\frac{1}{2}}),$ (11)

- *the global energy :* $\mathcal{E}^n = \dfrac{1}{2}(\,{}^t\mathbb{E}^n \mathbb{M}^\epsilon \mathbb{E}^n + \,{}^t\mathbb{H}^{n-\frac{1}{2}} \mathbb{M}^\mu \mathbb{H}^{n+\frac{1}{2}}).$ (12)

In the following, we shall prove that the global energy (12) is conserved through a time step and that it is a positive definite quadratic form of all unknowns under a CFL-like condition on the time-step Δt.

Lemma 1 *Using the DGTD-$\mathbb{P}_{p_i}$ method (9)-(10) for solving (1) with metallic boundaries only, the global discrete energy (12) is exactly conserved,* i.e. $\mathcal{E}^{n+1} - \mathcal{E}^n = 0, \; \forall \, n.$

Proof. We denote by $\mathbb{E}^{n+\frac{1}{2}} = \dfrac{\mathbb{E}^{n+1} + \mathbb{E}^n}{2}$. We have :

$$\mathcal{E}^{n+1} - \mathcal{E}^n = {}^t\mathbb{E}^{n+\frac{1}{2}}\mathbb{M}^\epsilon(\mathbb{E}^{n+1} - \mathbb{E}^n) + \frac{1}{2}\,{}^t\mathbb{H}^{n+\frac{1}{2}}\mathbb{M}^\mu(\mathbb{H}^{n+\frac{3}{2}} - \mathbb{H}^{n-\frac{1}{2}})$$

$$= \Delta t\,{}^t\mathbb{E}^{n+\frac{1}{2}}\mathbb{S}_N\mathbb{H}^{n+\frac{1}{2}} - \frac{1}{2}\Delta t\,{}^t\mathbb{H}^{n+\frac{1}{2}}(\,{}^t\mathbb{S}_N\mathbb{E}^{n+1} + \,{}^t\mathbb{S}_N\mathbb{E}^n)$$

$$= \Delta t\,{}^t\mathbb{H}^{n+\frac{1}{2}}(\,{}^t\mathbb{S}_N - \,{}^t\mathbb{S}_N)\mathbb{E}^{n+\frac{1}{2}} = 0.$$

This concludes the proof. □

Lemma 2 *Using the DGTD-$\mathbb{P}_{p_i}$ method (9)-(10), the global discrete electromagnetic energy $\mathcal{E}^n$ (12) is a positive definite quadratic form of all unknowns if:*

$$\Delta t \le \frac{2}{d_N}, \quad with \;\; d_N = \|\mathbb{M}^{\frac{-\mu}{2}}\,{}^t\mathbb{S}_N\mathbb{M}^{\frac{-\epsilon}{2}}\|, \tag{13}$$

where $\|.\|$ denotes a matrix norm, and the matrix $\mathbb{M}^{\frac{-\sigma}{2}}$ is the inverse square root of $\mathbb{M}^\sigma$. Also, for a given mesh, the stability limit of the LF_4 scheme is roughly 2.85 times larger than that of the LF_2 scheme.

Proof. The mass matrices $\mathbb{M}^\epsilon$ and $\mathbb{M}^\mu$ are symmetric positive definite and we can construct in a simple way their square root (also symmetric positive definite) denoted by $\mathbb{M}^{\frac{\epsilon}{2}}$ and $\mathbb{M}^{\frac{\mu}{2}}$ respectively.

Using the scheme (9) to develop $\mathbb{H}^{n+\frac{1}{2}}$ in function of $\mathbb{E}^n$ and $\mathbb{H}^{n-\frac{1}{2}}$, yields:

$$\mathcal{E}^n = \frac{1}{2}\,{}^t\mathbb{E}^n\mathbb{M}^\epsilon\mathbb{E}^n + \frac{1}{2}\,{}^t\mathbb{H}^{n-\frac{1}{2}}\mathbb{M}^\mu\mathbb{H}^{n+\frac{1}{2}}$$

$$= \frac{1}{2}\,{}^t\mathbb{E}^n\mathbb{M}^\epsilon\mathbb{E}^n + \frac{1}{2}\,{}^t\mathbb{H}^{n-\frac{1}{2}}\mathbb{M}^\mu\mathbb{H}^{n-\frac{1}{2}} - \frac{\Delta t}{2}\,{}^t\mathbb{H}^{n-\frac{1}{2}}\,{}^t\mathbb{S}_N\mathbb{E}^n$$

$$\geq \frac{1}{2}\|\mathbb{M}^{\frac{\epsilon}{2}}\mathbb{E}^n\|^2 + \frac{1}{2}\|\mathbb{M}^{\frac{\mu}{2}}\mathbb{H}^{n-\frac{1}{2}}\|^2 - \frac{\Delta t}{2}|\,{}^t\mathbb{H}^{n-\frac{1}{2}}\mathbb{M}^{\frac{\mu}{2}}\mathbb{M}^{\frac{-\mu}{2}}\,{}^t\mathbb{S}_N\mathbb{M}^{\frac{-\epsilon}{2}}\mathbb{M}^{\frac{\epsilon}{2}}\mathbb{E}^n|$$

$$\geq \frac{1}{2}\|\mathbb{M}^{\frac{\epsilon}{2}}\mathbb{E}^n\|^2 + \frac{1}{2}\|\mathbb{M}^{\frac{\mu}{2}}\mathbb{H}^{n-\frac{1}{2}}\|^2 - \frac{d_N\Delta t}{2}\|\mathbb{M}^{\frac{\mu}{2}}\mathbb{H}^{n-\frac{1}{2}}\|\|\mathbb{M}^{\frac{\epsilon}{2}}\mathbb{E}^n\|.$$

At this point, we choose to use an upper bound for the term $\|\mathbb{M}^{\frac{\mu}{2}}\mathbb{H}^{n-\frac{1}{2}}\|\|\mathbb{M}^{\frac{\epsilon}{2}}\mathbb{E}^n\|$ which might lead to sub-optimal lower bounds for the energy (and then to a slightly too severe stability limit for the scheme). Anyway, this stability limit is only sufficient, and not really close to necessary. We use the inequality:

$$\|\mathbb{M}^{\frac{\mu}{2}}\mathbb{H}^{n-\frac{1}{2}}\|\|\mathbb{M}^{\frac{\epsilon}{2}}\mathbb{E}^n\| \leq \frac{1}{2}(\|\mathbb{M}^{\frac{\mu}{2}}\mathbb{H}^{n-\frac{1}{2}}\|^2 + \|\mathbb{M}^{\frac{\epsilon}{2}}\mathbb{E}^n\|^2).$$

We then sum up the lower bounds for the $\mathcal{E}^n$ to obtain:

$$\mathcal{E}^n \geq \frac{1}{2}(1 - \frac{d_N\Delta t}{2})\|\mathbb{M}^{\frac{\epsilon}{2}}\mathbb{E}^n\|^2 + \frac{1}{2}(1 - \frac{d_N\Delta t}{2})\|\mathbb{M}^{\frac{\mu}{2}}\mathbb{H}^{n-\frac{1}{2}}\|^2.$$

Then, under the condition proposed in Lemma 2, the electromagnetic energy $\mathcal{E}^n$ is a positive definite quadratic form of all unknowns.

Moreover, for a given mesh, using the definition (10) of $\mathbb{S}_N$, the LF$_4$ scheme is stable if:

$$\Delta t\|\mathbb{M}^{\frac{-\mu}{2}}\,{}^t\mathbb{S}_4\mathbb{M}^{\frac{-\epsilon}{2}}\| \leq 2,$$

$$\Rightarrow \Delta t\|\mathbb{M}^{\frac{-\mu}{2}}\,{}^t(\mathbb{S}_2 - \frac{\Delta t^2}{24}\mathbb{S}_2\mathbb{M}^{-\mu}\,{}^t\mathbb{S}_2\mathbb{M}^{-\epsilon}\mathbb{S}_2)\mathbb{M}^{\frac{-\epsilon}{2}}\| \leq 2,$$

$$\Rightarrow |\Delta t d_2 - \frac{\Delta t^3}{24}d_2^3| \leq 2.$$

This inequality is verified if and only if $d_2\Delta t \leq 2(\sqrt[3]{2} + \sqrt[3]{4}) \simeq 2(2.847)$. This concludes the proof. $\qquad\square$

Now, our objective is to give an explicit CFL condition on Δt under which the local energy (11) is a positive definite quadratic form of the numerical unknowns $\mathbf{E}_i^n$ and $\mathbf{H}_i^{n-\frac{1}{2}}$. We first need some classical definitions.

Definition 2 *We assume that the tensors $\bar{\bar{\epsilon}}_i$ and $\bar{\bar{\mu}}_i$ are piecewise constant, i.e. $\bar{\bar{\epsilon}}_i = \epsilon_i$ and $\bar{\bar{\mu}}_i = \mu_i$. We denote by $c_i = 1/\sqrt{\epsilon_i\mu_i}$ the propagation speed in*

the finite element τ_i. We also assume that there exist dimensionless constants α_i and β_{ik} $(k \in \mathcal{V}_i)$ such that:

$$\forall \vec{\mathbf{X}} \in \mathcal{P}_i, \begin{cases} \|curl\, \vec{\mathbf{X}}\|_{\tau_i} \leq \dfrac{\alpha_i P_i}{V_i} \|\vec{\mathbf{X}}\|_{\tau_i}, \\[2mm] \|\vec{\mathbf{X}}\|_{a_{ik}}^2 \leq \dfrac{\beta_{ik} s_{ik}}{V_i} \|\vec{\mathbf{X}}\|_{\tau_i}^2, \end{cases} \tag{14}$$

where $\|\vec{\mathbf{X}}\|_{\tau_i}$ and $\|\vec{\mathbf{X}}\|_{a_{ik}}$ denote the L^2-norm of the vector field $\vec{\mathbf{X}}$ over τ_i and the interface a_{ik} respectively.

Lemma 3 *Using the LF_2 scheme (4)-(6)-(7), under assumptions of Definition 2, the local discrete energy $\mathcal{E}_i^n$ (11) is a positive definite quadratic form of all unknowns $(\mathbf{E}_i^n, \mathbf{H}_i^{n-\frac{1}{2}})$ and the scheme is stable if the time step Δt is such that:*

$$\forall i, \forall k \in \mathcal{V}_i, \quad c_i \Delta t [2\alpha_i + \beta_{ik}] < \frac{4 V_i}{P_i}, \tag{15}$$

(with the convention that, in the above formula, k should be replaced by i for a metallic boundary interface a_{ik}).

Proof. Using the scheme (3) to replace the occurrences of $\mathbf{H}_i^{n+\frac{1}{2}}$ in the definition of $\mathcal{E}_i$, and using the boundary fluxes given in (7), we get:

$$\mathcal{E}_i^n = \frac{\epsilon_i}{2} \|\mathbf{E}_i^n\|_{\tau_i}^2 + \frac{\mu_i}{2} \|\mathbf{H}_i^{n-\frac{1}{2}}\|_{\tau_i}^2 - \frac{\Delta t}{4} \mathbb{X}_i^n, \quad \text{with}$$

$$\mathbb{X}_i^n = \int_{\tau_i} \left(curl\, \vec{\mathbf{H}}_i^{n-\frac{1}{2}} \cdot \vec{\mathbf{E}}_i^n + curl\, \vec{\mathbf{E}}_i^n \cdot \vec{\mathbf{H}}_i^{n-\frac{1}{2}} \right) - \sum_{k \in \mathcal{V}_i} \int_{a_{ik}} (\vec{\mathbf{H}}_i^{n-\frac{1}{2}} \times \vec{\mathbf{E}}_k^n) \cdot \vec{n}_{ik}.$$

In the remainder of this proof, we omit the superscripts n and n-1/2 respectively in the electric and magnetic variables. We have the following identities:

$$|\mathbb{X}_i^n| \leq \|curl\, \vec{\mathbf{H}}_i\|_{\tau_i} \|\vec{\mathbf{E}}_i\|_{\tau_i} + \|curl\, \vec{\mathbf{E}}_i\|_{\tau_i} \|\vec{\mathbf{H}}_i\|_{\tau_i}$$

$$+ \frac{1}{2} \sum_{k \in \mathcal{V}_i} \left(\sqrt{\frac{\mu_i}{\epsilon_i}} \|\vec{\mathbf{H}}_i\|_{a_{ik}}^2 + \sqrt{\frac{\epsilon_i}{\mu_i}} \|\vec{\mathbf{E}}_k\|_{a_{ik}}^2 \right)$$

$$\leq \frac{2\alpha_i P_i}{V_i} \|\vec{\mathbf{H}}_i\|_{\tau_i} \|\vec{\mathbf{E}}_i\|_{\tau_i} + \frac{1}{2} \sum_{k \in \mathcal{V}_i} \left(\sqrt{\frac{\mu_i}{\epsilon_i}} \frac{\beta_{ik} s_{ik}}{V_i} \|\vec{\mathbf{H}}_i\|_{\tau_i}^2 + \sqrt{\frac{\epsilon_i}{\mu_i}} \frac{\beta_{ki} s_{ik}}{V_k} \|\vec{\mathbf{E}}_k\|_{\tau_k}^2 \right).$$

Noticing that $\|\vec{\mathbf{H}}_i\|_{\tau_i} \|\vec{\mathbf{E}}_i\|_{\tau_i} \leq \frac{c_i}{2} (\mu_i \|\vec{\mathbf{H}}_i\|_{\tau_i}^2 + \epsilon_i \|\vec{\mathbf{E}}_i\|_{\tau_i}^2)$, gathering all lower bounds for terms in the expression of $\mathcal{E}_i^n$ and using $P_i = \sum_{k \in \mathcal{V}_i} s_{ik}$ leads to:

$$\mathcal{E}_i^n \geq \sum_{k \in \mathcal{V}_i} \mathrm{s}_{ik} \left(\frac{1}{2P_i} - \frac{\alpha_i c_i \Delta t}{4V_i} \right) (\epsilon_i \|\vec{\mathbf{E}}_i\|_{\tau_i}^2 + \mu_i \|\vec{\mathbf{H}}_i\|_{\tau_i}^2)$$

$$- \frac{\Delta t}{8} \sum_{k \in \mathcal{V}_i} \mathrm{s}_{ik} \left(\sqrt{\frac{\mu_i}{\epsilon_i}} \frac{\beta_{ik}}{V_i} \|\vec{\mathbf{H}}_i\|_{\tau_i}^2 + \sqrt{\frac{\epsilon_i}{\mu_i}} \frac{\beta_{ki}}{V_k} \|\vec{\mathbf{E}}_k\|_{\tau_k}^2 \right).$$

Then, summing up these inequalities in order to obtain a lower bound for $\sum_i \mathcal{E}_i$ leads to an expression that we reorganize as sum over interfaces. We find that $\sum_i \mathcal{E}_i \geq \sum_{a_{ik}} \mathrm{s}_{ik} W_{ik}$ with:

$$W_{ik} = \epsilon_i \|\vec{\mathbf{E}}_i\|_{\tau_i}^2 \left(\frac{1}{2P_i} - \frac{\alpha_i c_i \Delta t}{4V_i} - \frac{\beta_{ik} c_i \Delta t}{8V_i} \right) +$$

$$\mu_i \|\vec{\mathbf{H}}_i\|_{\tau_i}^2 \left(\frac{1}{2P_i} - \frac{\alpha_i c_i \Delta t}{4V_i} - \frac{\beta_{ik} c_i \Delta t}{8V_i} \right) +$$

$$\epsilon_k \|\vec{\mathbf{E}}_k\|_{\tau_k}^2 \left(\frac{1}{2P_k} - \frac{\alpha_k c_k \Delta t}{4V_k} - \frac{\beta_{ki} c_k \Delta t}{8V_k} \right) +$$

$$\mu_k \|\vec{\mathbf{H}}_k\|_{\tau_k}^2 \left(\frac{1}{2P_k} - \frac{\alpha_k c_k \Delta t}{4V_k} - \frac{\beta_{ki} c_k \Delta t}{8V_k} \right).$$

Under the conditions proposed in Lemma 3, W_{ik} is a positive definite quadratic form of all unknowns and so is the local energy. This concludes the proof. $\square$

Note that, the existence of the constants α_i and β_{ik} ($k \in \mathcal{V}_i$) is always ensured. The values of α_i only depend on the local polynomial order p_i while the values of β_{ik} depend on p_i and on the number of hanging nodes on the interface a_{ik}. For instance, for orthogonal polynomials on a d-simplex $\beta_{ik} = (p_i+1)(p_i+d)/d$ (see [11]), and for arbitrary basis functions these values are given by:

$$\left(\frac{\alpha_i^2 P_i^2}{V_i^2}; \frac{\beta_{ik} \mathrm{s}_{ik}}{V_i} \right) = \left(\|\mathbf{M}^{-1/2} \mathbf{S_1} \mathbf{M}^{-1/2}\|; \|\mathbf{M}^{-1/2} \mathbf{S_2} \mathbf{M}^{-1/2}\| \right),$$

where $\mathbf{M}$ is the mass matrix without material parameter, $\mathbf{S_2} = 2S_{ik}$, and $\mathbf{S_1} = \int_{\tau_i} \mathrm{curl}\, \vec{\varphi}_{ij} \cdot \mathrm{curl}\, \vec{\varphi}_{il}$, $1 \leq j, l \leq d_i$.

4 Numerical experiments

We consider here the Maxwell equations in two space dimensions and in the TM-polarization; *i.e.* we solve for (H_x, H_y, E_z). We validate the theory by considering the propagation of an eigenmode which is a standing wave of frequency $f = 212$ MHz and wavelength $\lambda = 1.4$ m in a unitary metallic cavity

with $\epsilon = \mu = 1$ in normalized units. Owing to the existence of an exact analytical solution, this problem allows us to appreciate the numerical results at any point and time in the cavity. Numerical simulations make use of triangular meshes of the square $[0, 1] \times [0, 1]$ and a non-conforming mesh is obtained by locally refining (two refinement levels) the square zone $[0.25, 0.75] \times [0.25, 0.75]$ of a coarse conforming mesh as shown on Fig. 1. The resulting non-conforming mesh consists of 782 triangles and 442 nodes (36 of them are hanging nodes). For this non-conforming mesh, we assign to coarse (*i.e.* non refined) elements a high polynomial degree p_1 and to the refined region a low polynomial degree p_2. The resulting scheme is referred to as DGTD-$\mathbb{P}_{(p_1, p_2)}$. If $p_1 = p_2 = p$, the scheme is simply called DGTD-$\mathbb{P}_p$. Note that, for a conforming interface a_{ik},
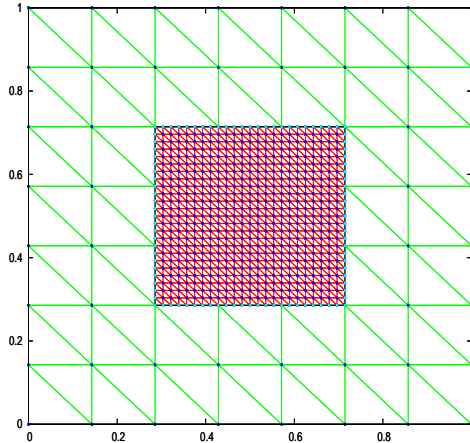

Fig. 1. Non-conforming locally refined triangular mesh.

the matrix S_{ik} defined in (5) can be evaluated in a direct way once and for all. However, for a non-conforming interface, we cannot calculate this matrix with an exact formula because it depends on the number of hanging nodes on the interface a_{ik}. For that, and only for non-conforming interfaces, we calculate the matrix S_{ik} by using a Gaussian quadrature formula. All simulations are carried out for time $t = 150$ which corresponds to 106 periods. In Tab. 1, we summarize the CFL values of the LF$_2$ DGTD-$\mathbb{P}_p$ method. If $p_1 \neq p_2$, the DGTD-$\mathbb{P}_{(p_1, p_2)}$ method has the same stability limit as the DGTD-$\mathbb{P}_{\min(p_1, p_2)}$ method, as long as the mesh is actually refined. We plot on Fig. 2 the time evolution of the overall L^2 error of the DGTD-$\mathbb{P}_p$ and DGTD-$\mathbb{P}_{(p_1, p_2)}$ methods using the LF$_2$ and LF$_4$ schemes. Tab. 2 gives the L^2 error, the number of degrees of freedom and the CPU time to reach time $t = 150$. It can be observed from Fig. 2 that the gain in the L^2 error is noticeable when the accuracy in space and time is increased. Moreover, it is clear from (6) and Lemma 2 that, for the same non-conforming mesh, each time step of LF$_4$ requires 2 times more memory than the LF$_2$ time step, but its stability limit is almost 2.85 times less restrictive. Then, LF$_4$ requires almost 1.5 times less CPU time and is roughly 15 times more efficient than LF$_2$. Furthermore, for a given accuracy, the LF$_4$ DGTD-$\mathbb{P}_{(p_1, p_2)}$ method requires less CPU time than the LF$_4$ DGTD-$\mathbb{P}_p$ method. Fig. 3 illustrates the numerical convergence of the DGTD-

11

$\mathbb{P}_p$ and DGTD-$\mathbb{P}_{(p_1,p_2)}$ methods. Corresponding asymptotic convergence orders are summarized in Tab. 3. As it could be expected from the use of the Nth accurate time integration scheme, the asymptotic convergence order is bounded by N independently of the interpolation degree.

Table 1

The CFL values of the LF$_2$ DGTD methods.

DGTD-$\mathbb{P}_p$ method, $\quad p =$	**1**	**2**	**3**	**4**	**5**
CFL(LF$_2$)	0.3	0.2	0.1	0.08	0.06

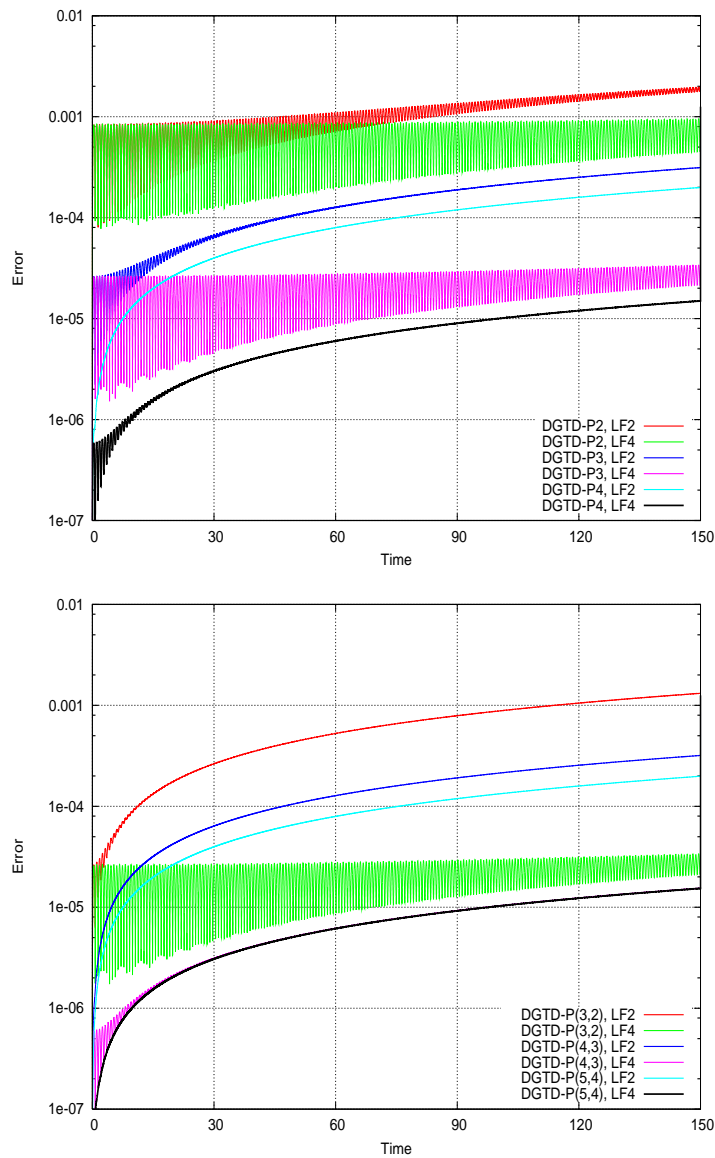| DGTD-$\mathbb{P}_{(p_1,p_2)}$ method, $\quad (p_1, p_2) =$	**(3,2)**	**(4,2)**	**(4,3)**	**(5,3)**	**(5,4)**
CFL(LF$_2$)	0.2	0.2	0.1	0.1	0.08

Fig. 2. Time evolution of the L^2 error.
DGTD-$\mathbb{P}_p$ (top) and DGTD-$\mathbb{P}_{(p_1,p_2)}$ (bottom) methods.

Table 2
DOF, L^2 errors and CPU time in minutes using the LF$_2$ and LF$_4$ DGTD methods.

DGTD-$\mathbb{P}_p$ method		LF$_2$		LF$_4$	
p	# DOF	Error	CPU (min)	Error	CPU (min)
2	4692	1.8E-03	11	5.5E-04	8
3	7820	3.1E-04	39	2.4E-05	28
4	11730	1.9E-04	98	1.5E-05	70
5	16422	1.5E-04	220	1.3E-05	155

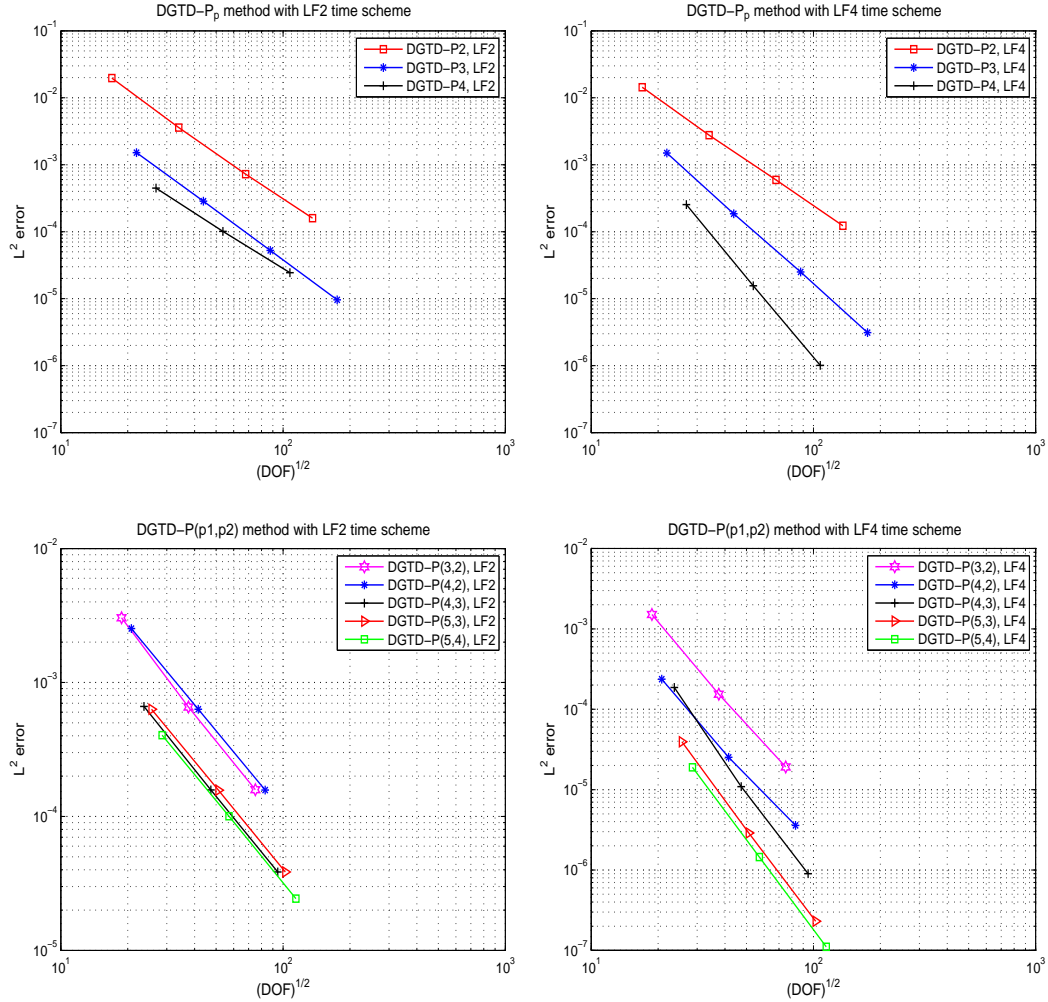| DGTD-$\mathbb{P}_{(p_1,p_2)}$ method		LF$_2$		LF$_4$	
(p_1,p_2)	# DOF	Error	CPU (min)	Error	CPU (min)
(3,2)	6668	1.3E-03	17	2.3E-05	12
(4,2)	9138	1.3E-03	27	1.5E-05	19
(4,3)	10290	3.2E-04	61	1.5E-05	44
(5,4)	14694	2.0E-04	134	1.4E-05	95

Fig. 3. Numerical convergence of the DGTD-$\mathbb{P}_p$ and DGTD-$\mathbb{P}_{(p_1,p_2)}$ methods.

Table 3

Asymptotic convergence orders of the LF$_2$ and LF$_4$ DGTD methods.

DGTD-$\mathbb{P}_p$ method, $p =$	2	3	4
LF$_2$ scheme	2.28	2.33	2.10
LF$_4$ scheme	2.32	2.97	3.99

DGTD-$\mathbb{P}_{(p_1,p_2)}$ method, $(p_1,p_2) =$	(3,2)	(4,2)	(4,3)	(5,3)	(5,4)
LF$_2$ scheme	2.13	2.00	2.05	2.02	2.03
LF$_4$ scheme	3.15	3.02	3.85	3.71	3.71

5   Concluding remarks

In this paper, we have studied a high-order discontinuous Galerkin method for the discretization of the time-domain Maxwell equations on non-conforming simplicial meshes. We proved that the method conserves a discrete equivalent of the electromagnetic energy and it is stable under some CFL-type stability condition. Numerical simulations were performed by considering an eigenmode problem in two space dimensions. We have shown that, for a given non-conforming mesh, the DGTD methods coupled to the LF$_4$ scheme is at least 15 times more accurate and requires roughly 1.5 times less CPU time than the LF$_2$ DGTD methods. Concerning future works, our objective is to design a truly hp-adaptive method through the construction of an appropriate error estimator.

References

[1] M. Bernacki, L. Fezoui, S. Lanteri, and S. Piperno. Parallel unstructured mesh solvers for heterogeneous wave propagation problems. Appl. Math. Model., 30:744–763, 2006.

[2] F. Collino, T. Fouquet, and P. Joly. Conservative space-time mesh refinement methods for the FDTD solution of Maxwell's equations. J. Comput. Phys., 211:9–35, 2006.

[3] G. Cohen, X. Ferrieres, and S. Pernet. A spatial high-order hexahedral discontinuous Galerkin method to solve Maxwell's equations in time domain. J. Comput. Phys., 217:340–363, 2006.

[4] H. Fahs. Development of a hp-like discontinuous Galerkin time-domain method on non-conforming simplicial meshes for electromagnetic wave propagation. Int. J. Numer. Anal. Model., 6:193–216, 2009.

[5] L. Fezoui, S. Lanteri, S. Lohrengel, and S. Piperno. Convergence and stability of a discontinuous Galerkin time-domain method for the heterogeneous Maxwell

equations on unstructured meshes. ESAIM: Math. Model. and Numer. Anal., 39:1149–1176, 2005.

[6] J.S. Hesthaven and T. Warburton. Nodal high-order methods on unstructured grids. I. Time-domain solution of Maxwell's equations. J. Comput. Phys., 181:186–221, 2002.

[7] D. Kopriva, S.L. Woodruff, and M.Y. Hussaini. Discontinuous spectral element approximation of Maxwell's equations. In B. Cockburn, G.E. Karniadakis, and C.W. Shu, editors, *Discontinuous Galerkin Methods: Theory, Computation and Applications*, vol. 11, Springer-Verlag, 2000, pp. 355–362.

[8] G. Scarella, O. Clatz, S. Lanteri, G. Beaume, S. Oudot, J.-P. Pons, S. Piperno, P. Joly, and J. Wiart. Realistic numerical modelling of human head tissue exposure to electromagnetic waves from cellular phones. Comptes Rendus Physique, 7:501–508, 2006.

[9] H. Spachmann, R. Schuhmann, and T. Weiland. High order explicit time integration schemes for Maxwell's equations. Int. J. Numer. Model., 15:419–437, 2002.

[10] A. Taflove. *Advances in computational electrodynamics, the finite-difference time-domain method*. Artech House, Boston, London, 1998.

[11] T. Warburton and J.S. Hesthaven. On the constants in *hp*-finite element trace inverse inequalities. Comput. Methods Appl. Mech. Engrg., 192:2765–2773, 2003.

[12] T. Xiao and Q.H. Liu. A staggered upwind embedded boundary (SUEB) method to eliminate the FDTD staircasing error. IEEE Trans. Antennas and Propagat., 52:730–741, 2004.

[13] K.S. Yee. Numerical solution of initial boundary value problems involving Maxwell's equations in isotropic media. IEEE Trans. Antennas and Propagat., 14:302–307, 1966.

[14] A. Yefet and P.G. Petropoulos. A staggered fourth-order accurate explicit finite difference scheme for the time-domain Maxwell's equations. J. Comput. Phys., 168:286–315, 2001.

[15] J.L. Young. High-order, leapfrog methodology for the temporally dependent Maxwell's equations. Radio Science, 36:9–17, 2001.